Ultrasensitive thermal sensors based on whispering gallery modes in a polymer core optical ring resonator

Nai Lin,[1] Lan Jiang,[1,*] Sumei Wang,[1] Hai Xiao,[2] Yongfeng Lu,[3] and Hailung Tsai[4]

[1]Laser Micro/Nano Fabrication Laboratory, School of Mechanical Engineering, Beijing Institute of Technology, 100081, China

[2]Department of Electrical and Computer Engineering, Missouri University of Science and Technology, Rolla, Missouri 65409, USA

[3]Department of Electrical Engineering, University of Nebraska-Lincoln, Lincoln, Nebraska 68588-0511, USA

[4]Department of Mechanical and Aerospace Engineering, Missouri University of Science and Technology, Rolla, Missouri 65409, USA

*Corresponding author: jianglan@bit.edu.cn

Received 31 May 2011; revised 25 July 2011; accepted 26 August 2011; posted 29 August 2011 (Doc. ID 148485); published 17 November 2011

This study proposes a thermal sensor based on whispering gallery modes (WGMs) in a polymer core optical ring resonator (PCORR). The thermal sensitivity and detection limit (i.e., the temperature resolution) for WGMs of various orders and polarizations are theoretically studied as a function of the ring wall thickness. The results show that the temperature detection limits can be as low as 4×10^{-5} and 6×10^{-6} K for laser linewidths of 2 and 0.3 MHz, respectively. The ultrahigh temperature resolution makes the PCORR a very promising platform for temperature measurement. The analysis also shows that the WGM of a lower order has better thermal sensing performance and a thinner optimal thickness of the ring resonator.

OCIS codes: 140.4780, 230.5750, 280.4788, 160.5470.

1. Introduction

Many research activities have been focused on optical microresonators with whispering gallery modes (WGMs) for broad applications, such as low-threshold lasers [1], cavity quantum electrodynamics [2], high-resolution spectroscopy [3], and refractive index sensors [4–6]. Most of the applications require thermal stability control because the WGMs are susceptible to thermal fluctuations, including the environmental temperature variations and probe-induced energy absorptions. Optical polymer coatings of negative thermal refraction coefficients have been proposed to compensate the WGM thermal drift of silica microresonators [7–9]. On the other hand, the ultrasensitive shift of the WGM resonance to the ambient temperature can be used to design highly sensitive thermal sensors. Especially due to the high Q factors of the WGM resonances, the smallest measurable temperature change (i.e., the detection limit) can be significantly enhanced compared with conventional thermal sensors. For example, Ma *et al.* report a silica-microsphere-based thermal sensor by measuring the WGM resonance shift in the transmission spectrum [10,11]. The Q factors of silica microresonators are ultrahigh, because the absorption loss of light in silica is very low [12]. But, due to the small thermal nonlinearity of silica, the thermal sensitivity

0003-6935/11/336254-07$15.00/0

of the silica-microresonator-based thermal sensor is relatively low.

Most recently, there has been increasing interest in the research of polymers for high-sensitivity thermal sensing. Polymers such as polydimethyl siloxane (PDMS), polymethyl methacrylate, and polystyrene have much larger thermal effect than silica, which provides the high sensitivity for temperature measurement. For instance, the study by Li *et al.* proved that the thermal sensitivity of a silica microresonator can be enhanced by coating a surface layer of PDMS, and the temperature detection limit of the PDMS-coated silica resonator can be as low as 1×10^{-4} K [13]. Another interesting approach would be to fabricate microresonators using polymers only, without a silica master. Dong *et al.* demonstrated a PDMS-microsphere-based thermal sensor with an ultrahigh sensitivity of 245 pm/K in the 1480 nm band [14]. However, the Q factors of the polymer-coated or polymer resonators are lower than that of the silica resonators, because the absorption loss of light in polymer is much larger than that in silica, especially in the infrared band (~1 dB/cm at the wavelength around 1550 nm) [15]. In addition, the WGM responses to the positive thermal expansion and the negative thermal refraction of the polymer are opposite and counteract with each other, which limits the further improvement of the thermal sensitivity.

This study proposes a thermal sensor based on a polymer core optical ring resonator (PCORR), as shown in Fig. 1. Similar to the PDMS-microsphere-based thermal sensors [14], the positive thermal expansion effect of the PCORR is dominant in thermal sensing, and is partly compensated by the negative thermal refraction of polymer for an ultrathin silica capillary. But, by increasing the wall thickness of the silica capillary, the WGM energy can be mostly distributed in silica, which reduces (or even eliminates) the negative thermal refraction effect of polymer and finally improves the thermal sensitivity. Furthermore, when the WGM energy mostly distributes in the silica capillary, the Q factor is further improved because of much smaller absorption loss of silica than polymer. Because of both high thermal sensitivity and high Q factor, the temperature detection limit of the proposed thermal sensor can be further enhanced compared with previous approaches using WGM resonators for thermal sensing.

The PCORR can be fabricated by applying the polymer materials into the core of a fused silica or aluminosilicate glass capillary. The WGMs excited in such capillary resonators have been both theoretically and experimentally investigated [16–18]. Also, the polymer materials have been successfully integrated with WGM resonators of various shapes [9,13,18,19]. These works provide a basis for the implementation of the proposed sensor. This study performs a detailed theoretical analysis of the thermal sensing performance of the proposed sensor. The theory and numerical models to analyze the thermal sensitivity and detection limit are presented in Section 2. Based on the models, the thermal responses of the WGMs of different polarizations and orders are studied as a function of the ring wall thickness in Section 3. Major results are reported in Section 4.

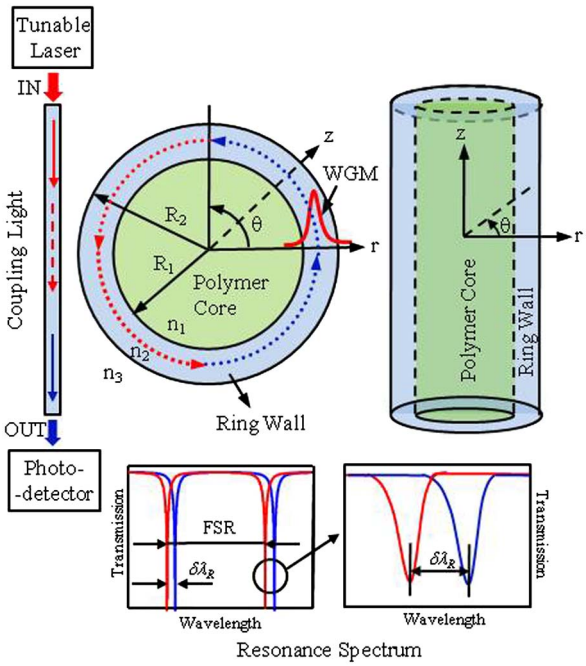

Fig. 1. (Color online) Polymer core ring resonator (PCORR)-based thermal sensor configuration. The PCORR is shown in cylindrical coordinates (r, θ, and z). n_1, n_2, and n_3 are the refractive indices of the polymer core, ring wall and surrounding medium, respectively. FSR is defined as the difference between two adjacent resonant wavelengths. $\delta\lambda_R$ denotes the resonance shift induced by the temperature change.

2. Theory and Numerical Models

In the common measurement setup for a WGM-based sensor, the optical source (DFB laser or external-cavity laser) is tuned over a very small spectral range (typically on the order of pm). The tunable laser is coupled into the microresonator through a waveguide (e.g., a fiber taper), which also couples light out of the PCORR. When the laser wavelength matches the WGM resonant condition, the light couples into the microresonator and causes a spectral dip (usually a Lorentzian-shaped resonance) in the measured transmission spectrum detected by a photodetector. A temperature change would induce changes in the optical and size parameters of the PCORR (including both the polymer core and the silica or aluminosilicate ring wall), which finally leads to a resonance shift in the transmission spectrum ($\delta\lambda_R$ in Fig. 1). Hence, by measuring the wavelength shift, it is possible to estimate the change of the surrounding temperature.

Over the years, the WGM modal structures and resonance spectra of ring resonators have been well and widely studied [20–22]. In general, the WGM resonance spectrum is determined by the size of

the resonator and the refractive index inside/outside the resonator. Considering a ring resonator with inner radius R_1 and outer radius R_2 (as shown in Fig. 1), the characteristic equation to specify the resonant wavelengths λ_R of the WGMs can be expressed by [21,22]

$$N_0 \frac{H_m'^{(1)}(k_0 n_3 R_2)}{H_m^{(1)}(k_0 n_3 R_2)} = \frac{B_m J_m'(k_0 n_2 R_2) + H_m'^{(1)}(k_0 n_2 R_2)}{B_m J_m(k_0 n_2 R_2) + H_m^{(1)}(k_0 n_2 R_2)},$$
$$N_0 = \begin{cases} n_2/n_3, & \text{TE modes} \\ n_3/n_2, & \text{TM modes} \end{cases}, \quad (1)$$

where $k_0 = 2\pi/\lambda_R$ is the resonant wave vector, TE modes and TM modes denote the WGMs with magnetic fields and electric fields along the cylinder longitudinal direction, respectively, m is the angular mode number of the WGMs, J_m and $H_m^{(1)}$ are the mth Bessel function and the mth Hankel function of the first kind, respectively, and B_m is a coefficient and its expression is given by

$$B_m = \frac{N_1 J_m(k_0 n_1 R_1) H_m'^{(1)}(k_0 n_2 R_1) - J_m'(k_0 n_1 R_1) H_m^{(1)}(k_0 n_2 R_1)}{J_m'(k_0 n_1 R_1) J_m(k_0 n_2 R_1) - N_1 J_m(k_0 n_1 R_1) J_m'(k_0 n_2 R_1)}, \qquad N_0 = \begin{cases} n_1/n_2, & \text{TE modes} \\ n_2/n_1, & \text{TM modes} \end{cases}. \quad (2)$$

For a specific number of m, there is a series of λ_R that satisfies the characteristic equation. In the decreasing value of λ_R, these resonant modes are called the first-order mode, the second-order mode..., the lth-order mode, and so on. A temperature variation of δT causes a change in the polymer core radius and the ring wall thickness through the thermal expansion effect, and also a change in the refractive indices of the polymer core and the ring wall through the thermal refraction effect [8]:

$$R_1' = R_1(1 + \alpha_1 \delta T), \qquad h' = h(1 + \alpha_2 \delta T),$$
$$n_i' = n_i + (dn_i/dT)\delta T, \quad (3)$$

where $h = R_2 - R_1$ is ring wall thickness, R_1' and h' are the core radius and the ring wall thickness after a temperature change, α_1 and α_2 are linear thermal expansion coefficients of the polymer core and the ring wall, respectively, n_i' is the refractive index of the corresponding material after temperature change, and dn_i/dT is the thermal refraction coefficient of the corresponding material. By substituting Eq. (3) into Eq. (1), the temperature-variation-induced resonant wavelength shift $\delta\lambda_R$ can be numerically calculated. But, from the characteristic equation alone, it is difficult to derive an explicit formula of the thermal sensitivity to describe the relation between $\delta\lambda_R$ and δT. The thermal sensitivity of the resonant wavelength shift versus temperature change can be given by [13]

$$S = \frac{\delta\lambda_R}{\delta T} = \lambda_R \left(\frac{1}{n_{\text{eff}}} \frac{dn_{\text{eff}}}{dT} + \alpha \right), \quad (4)$$

where n_{eff} is the effective refractive index of the WGMs, which can be approximately expressed as $n_{\text{eff}} = \eta_1 n_1 + \eta_2 n_2 + \eta_3 n_3$. η_1, η_2, and η_3 denote the fractions of light energy distributed in the polymer core, the ring wall and the surrounding medium, respectively, and α is the linear thermal expansion coefficient of the whole ring resonator, and for a thin-walled ring resonator it can be approximated by

$$\alpha = \frac{\alpha_1 R_1 + \alpha_2 h}{R_2}. \quad (5)$$

So, the thermal sensitivity is further expressed as

$$S \approx \lambda_R \left(\frac{\sum_{i=1}^{3} \eta_i (dn_i/dT)}{\sum_{i=1}^{3} (\eta_i n_i)} + \frac{\alpha_1 R_1 + \alpha_2 h}{R_2} \right). \quad (6)$$

The energy fractions can be calculated by

$$\eta_i = \begin{cases} \frac{I_i}{I_1 + I_2 + I_3}, & \text{TE Modes} \\ \frac{n_i^2 I_i}{n_1^2 I_1 + n_2^2 I_2 + n_3^2 I_3}, & \text{TM Modes} \end{cases}, \qquad i = 1, 2, 3, \quad (7)$$

where

$$I_1 = \int_0^{R_1} |A_m J_m(k_0 n_1 r)|^2 \mathrm{d}_r,$$
$$I_3 = \int_{R_2}^{\infty} |C_m H_m^{(1)}(k_0 n_3 r)|^2 \mathrm{d}_r,$$
$$I_2 = \int_{R_1}^{R_2} |B_m J_m(k_0 n_2 r) + H_m^{(1)}(k_0 n_2 r)|^2 \mathrm{d}_r. \quad (8)$$

A_m and C_m are the coefficients determined by

$$A_m = \frac{B_m J_m(k_0 n_2 R_1) + H_m^{(1)}(k_0 n_2 R_1)}{J_m(k_0 n_1 R_1)},$$
$$C_m = \frac{B_m J_m(k_0 n_2 R_2) + H_m^{(1)}(k_0 n_2 R_2)}{H_m^{(1)}(k_0 n_3 R_2)}. \quad (9)$$

By substituting Eq. (7) into Eq. (6), the thermal sensitivity for the TE and TM modes in the ring resonators can be, respectively, expressed by

$$S_{\mathrm{TE}} \approx \lambda_R \left(\frac{\sum_{i=1}^{3} I_i (dn_i/dT)}{\sum_{i=1}^{3} (I_i n_i)} + \frac{\alpha_1 R_1 + \alpha_2 h}{R_2} \right),$$
$$S_{\mathrm{TM}} \approx \lambda_R \left(\frac{\sum_{i=1}^{3} I_i n_i^2 (dn_i/dT)}{\sum_{i=1}^{3} (I_i n_i^3)} + \frac{\alpha_1 R_1 + \alpha_2 h}{R_2} \right). \quad (10)$$

The detection limit of temperature, defined as the smallest measurable temperature change $(\delta T)_{\min}$, is calculated by [13]

$$(\delta T)_{\min} = \frac{(\delta\lambda_R)_{\min}}{\Delta\lambda_R} \times \frac{\lambda_R}{Q \times S}, \quad (11)$$

where $(\delta\lambda_R)_{\min}$ is the minimum resolvable wavelength shift of the detector, and $\Delta\lambda_R$ is the linewidth of the resonance. The value of $(\delta\lambda_R)_{\min}/\Delta\lambda_R$ is limited by the detector noise, including the thermal noise and the shot noise of the detector. The Q factor of the ring resonator is determined by the lumped loss of light in the resonator, which includes the tunneling loss (also known as radiation loss), the scattering loss from surface irregularities, and the material absorption loss [21]. Tunneling loss is due to the curvature of the waveguiding boundaries in the direction of propagation, and it is very low for the microresonator with a large radius. Thus, the total Q factor can be further expressed as

$$\frac{1}{Q} \approx \frac{1}{Q_{\mathrm{sca}}} + \frac{1}{(Q_{\mathrm{abs}})_{\mathrm{wall}}} + \frac{1}{(Q_{\mathrm{abs}})_{\mathrm{core}}}, \quad (12)$$

where $1/Q_{\mathrm{sca}}$ denotes the scattering loss, and $1/(Q_{\mathrm{abs}})_{\mathrm{wall}}$ and $1/(Q_{\mathrm{abs}})_{\mathrm{core}}$ denote the material absorption loss of light in the ring wall and the polymer core, respectively. $(Q_{\mathrm{abs}})_{\mathrm{core}}$ can be further calculated by $(Q_{\mathrm{abs}})_{\mathrm{core}} = 2\pi n_1/(\lambda_R \sigma \eta_1)$ [12], where σ is the optical attenuation coefficient of the polymer core. In practical applications of thermal sensors, various noises (including the detector thermal noise and shot noise) can perturb the resonance spectrum [13]. In these cases, the accurate detection of the resonant wavelength shift is difficult for a broad resonance linewidth, which suggests that a narrow resonance (thus a high Q factor) is preferred to achieve good detection performance.

3. Design and Optimization of the Thermal Sensor

In the simulation, the refractive indices are chosen as $n_1 = 1.41$ for the polymer core (consisting of PDMS), $n_2 = 1.45$ for the fused silica ring wall, and $n_3 = 1.0$ for the air outside the ring resonator. PDMS is a conventional optical polymer whose thermal expansion coefficient and thermal refraction coefficient are about $\alpha_1 = 2.70 \times 10^{-4}/\mathrm{K}$ and $dn_1/dT = -1.0 \times 10^{-4}/\mathrm{K}$, respectively [14]. The thermal expansion coefficient and thermal refraction coefficient of fused silica are about $\alpha_2 = 5.5 \times 10^{-7}/\mathrm{K}$ and $dn_2/dT = 1.19 \times 10^{-5}/\mathrm{K}$, respectively [8]. The material optical parameters are chosen at room temperature and at the wavelength around 1550 nm. Figure 2 shows the thermal sensitivity for both TE and TM modes of the first three orders, as a function of the ring wall thickness. Similarly with other shapes of optical microresonators (e.g., microspheres, microdisks, and microtoroids), the diameter of the microcapillary resonators is only a few tens or a few hundreds of micrometers [23]. In this study, the original outer radius of the ring resonator before temperature change is kept at $R_2 = 50\,\mu\mathrm{m}$ for all cases, and the angular mode numbers m are chosen to keep the resonant wavelength around 1550 nm. It is shown that the thermal sensitivity basically increases with the ring wall thickness until it reaches the highest value S_{MAX}, which is marked by the symbols in Fig. 2. This is because the positive thermal expansion of the whole resonator is dominant, and it is partly compensated by its negative thermal refraction for an ultrathin wall thickness. When the wall thickness increases, the light energy in the polymer core decreases (i.e., η_1 decreases). Then, according to Eq. (6), the resonance response to the polymer negative thermal refraction becomes smaller and finally leads to an increase in the thermal sensitivity. As shown in Fig. 3, at $h = 1$ and $2\,\mu\mathrm{m}$, the energy fractions of the first-order TM mode in the polymer are $\eta_1 = 0.34$ and 0.04, which correspond to thermal sensitivities of ~382 and ~410 pm/K, respectively. At the same wall thickness, the WGM of a higher order has a larger value of η_1 and thus corresponds to a smaller thermal sensitivity.

Figure 2 also shows that the value of S_{MAX} decreases as the WGM order increases, and it needs a larger wall thickness to achieve S_{MAX} for a WGM of a higher order. For instance, S_{MAX} is about 398 and 388 pm/K at $h = 3.5$ and $4.75\,\mu\mathrm{m}$ for the second- and third-order TM modes, respectively. For WGMs of the same order, the thermal sensitivity of the TE mode is slightly smaller than that of the TM mode. When the ring wall thickness increases further to $\eta_1 \approx 0$, $\eta_1 n_1$ and $\eta_3 n_3$ are negligible compared with

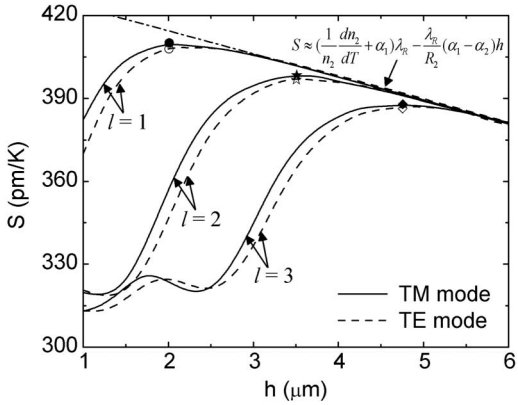

Fig. 2. Thermal sensitivity S for TM modes (solid curves) and TE modes (dashed curves) of the first three orders as a function of the ring wall thickness h. The symbols denote the highest thermal sensitivity S_{MAX} for the $\mathrm{TM}_{l=1}$ (solid circle), $\mathrm{TE}_{l=1}$ (open circle), $\mathrm{TM}_{l=2}$ (solid star), $\mathrm{TE}_{l=2}$ (open star), $\mathrm{TM}_{l=3}$ (solid diamond), and $\mathrm{TE}_{l=3}$ (open diamond) modes, respectively.

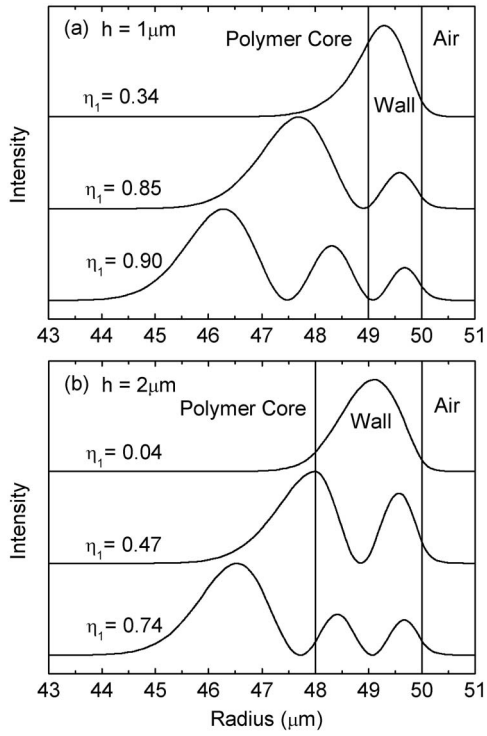

Fig. 3. Light energy intensity distribution along the radial direction for TM modes of the first three orders, at (a) $h = 1$ and (b) $2\,\mu$m.

$\eta_2 n_2$ in Eq. (6), and thus the thermal sensitivity can be further evaluated by

$$S \approx \left(\frac{1}{n_2}\frac{dn_2}{dT} + \alpha_1\right)\lambda_R - \frac{\lambda_R}{R_2}(\alpha_1 - \alpha_2)h, \qquad (13)$$

where S decreases linearly with h. Figure 4 shows the resonant wavelength shift as a function of temperature change. The curves represent the approximate results evaluated by $\delta\lambda_R = S \times \delta T$, and the symbols denote the accurate results that are numerically calculated by substituting Eq. (3) into Eq. (1). From Fig. 4, the proposed thermal sensor exhibits

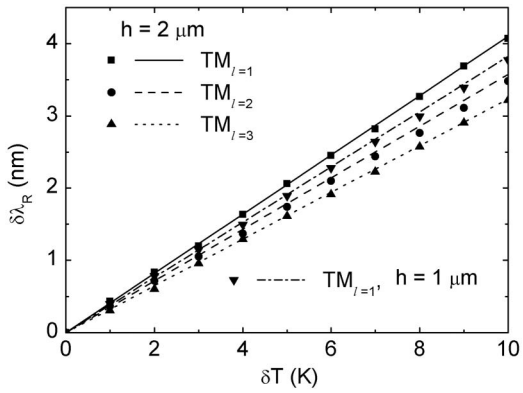

Fig. 4. Resonant wavelength shift $\delta\lambda_R$ for TM modes of different orders as a function of the temperature change δT at $h = 1$ and $2\,\mu$m.

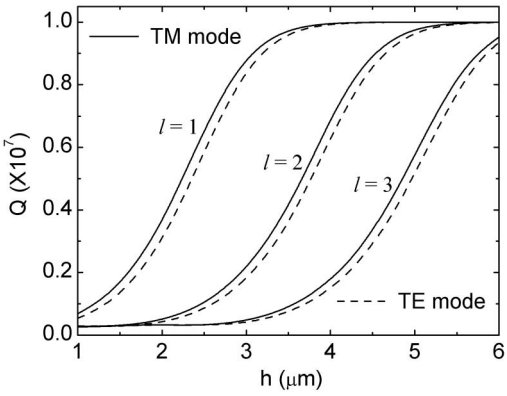

Fig. 5. Q factors for TM modes (solid curves) and TE modes (dashed curves) of the first three orders as a function of the ring wall thickness h.

an excellent linear sensing characteristic and the curves are in agreement with the accurate values.

The aforementioned analysis shows that the thermal sensitivity of the proposed thermal sensor is very high. Also, the Q factor of the PCORR can be very high, as shown in Fig. 5. The Q factor limited by the scattering loss and the absorption loss of silica is taken to be around 10^7 [21], and the optical attenuation coefficient of the polymer is about $\sigma = 1\,\mathrm{dB/cm}$ (i.e., $0.23\,\mathrm{cm^{-1}}$) at a wavelength around 1550 nm [15]. As the ring wall thickness increases, the light energy in the polymer core is gradually transferred into the silica wall, and thus the Q factor increases due to the much smaller absorption loss of silica than polymer until it reaches 10^7. Figure 5 also shows that the Q factor of the TE mode is slightly lower than that of the TM mode of the same order.

Figure 6 shows the temperature detection limit as a function of the ring wall thickness. The value of $(\delta\lambda_R)_{\min}/\Delta\lambda_R$ limited by the detector noise is assumed to be about 1/100 [13]. It is shown that, as the ring wall thickness increases, the temperature detection limit decreases quickly until it reaches the minimum, at which the Q factor reaches 10^7. When the ring wall thickness increases further, the detection

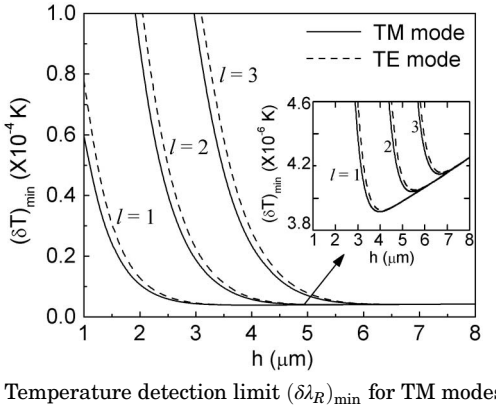

Fig. 6. Temperature detection limit $(\delta\lambda_R)_{\min}$ for TM modes (solid curves) and TE modes (dashed curves) of the first three orders as a function of the ring wall thickness h. The value of $(\delta\lambda_R)_{\min}/\Delta\lambda_R$ limited by the detector noise is assumed to be 1/100.

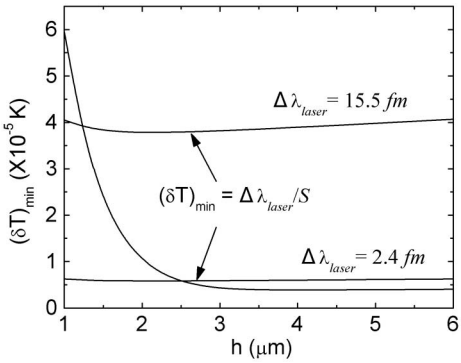

Fig. 7. Temperature detection limit of the first-order TM mode restricted by laser linewidths of 15.5 and 2.4 fm, respectively, as a function of the ring wall thickness h.

limit increases slightly due to the decreased thermal sensitivity (as shown in Fig. 2). The theoretical predication of the minimum temperature detection limit is as low as $\sim 4 \times 10^{-6}$ K for the WGMs of the first three orders. But, in practical applications of the thermal sensor, the temperature detection limit might be further restricted by the linewidth of the detection laser ($\Delta\lambda_{\text{laser}}$) [11], which can be given by $(\delta T)_{\text{min}} = \Delta\lambda_{\text{laser}}/S$. Figure 7 shows the temperature detection limit of the first-order TM mode after considering the restriction of the laser linewidth. A distributed feedback (DFB) laser with a linewidth of 2 MHz [11] and an external-cavity laser with a linewidth of 0.3 MHz [14] are considered. At a wavelength around 1550 nm, 2 and 0.3 MHz are equivalent to about 15.5 and 2.4 fm. From Fig. 7, the temperature detection limit of the first-order TM mode can be as low as $\sim 6 \times 10^{-6}$ K for a laser linewidth of 2.4 fm, which is about one order smaller than that ($\sim 4 \times 10^{-5}$ K) for a laser linewidth of 15.5 fm. So, the detection laser of a narrower linewidth could be implemented to achieve a lower detection limit in practice. The state-of-the-art laser technology has pushed the laser linewidth to a few kilohertz, which makes it possible to reach the smallest theoretical prediction of the temperature detection limit.

In addition to the thermal sensitivity and detection limit, it is desirable to have a wider free spectral range (FSR in Fig. 1). FSR is defined as the difference between two adjacent resonant wavelengths of the same order. A small FSR might impose a limitation on the dynamic range of the temperature measurement as it becomes difficult to differentiate the corresponding mode number of the resonance peaks. Calculated by Eq. (1), the FSR of all the modes in the PCORR with an outer radius of 50 μm is about 5.5 nm, which corresponds to a temperature variation of 13–18 K for thermal sensitivity between 310 and 412 pm/K (in Fig. 2). However, in practical applications of WGM-based sensors, the WGM resonance spectrum is not strictly periodical, and thus the practical detectable temperature variations can be much larger than the FSR [24]. Moreover, the capillary resonators can be integrated with planar waveguide structures on a chip to form a two-dimensional array for multiplexed detection [23], which could further increase the detection range of temperature changes. A drawback of the proposed thermal sensor is its operating range (223.15–437.15 K), limited by the PDMS transition temperature [14].

4. Conclusions and Discussion

This study proposes a thermal sensor by applying polymer material into the core of a ring resonator. Temperature variation causes changes in both optical and size parameters of the resonator materials, which are detected as the resonance spectral shift. By increasing the wall thickness of the silica capillary, the WGM energy distributed in polymer can be transferred into silica, and the negative thermal refraction effect of polymer is reduced or even eliminated, which finally leads to an enhancement of the thermal sensitivity. For WGMs of the first three orders around 1550 nm, the highest thermal sensitivity is larger than ~380 pm/K. The Q factor is also improved as the silica capillary thickness increases, because the material absorption loss of light in silica is much smaller than that in polymer. The detection limit of the proposed thermal sensor can be as low as $\sim 6 \times 10^{-6}$ K for a laser linewidth of 0.3 MHz, which is obviously enhanced compared with previous approaches using WGM resonators for thermal sensing (greater than $\sim 1 \times 10^{-4}$ K) [10,11,13,14,24]. While some of the reported interferometric temperature sensors have better sensitivities (0.99–3.195 nm/K), their temperature detection limits (3.4×10^{-3}–0.4 K) are much larger than that of the thermal sensors based on WGM resonators of high Q factors [14].

This study considers PDMS as the polymer material filled in the silica capillary, and the thermal expansion coefficient of PDMS is much larger than that of silica. After the temperature increases, the polymer core will expand and press against the silica capillary. As a result, the practical thermal expansion coefficient of the polymer core, α_1, might be smaller than the reference value of 2.70×10^{-4}/K [14] for a thick-walled silica capillary. In addition, the thermal expansion coefficient of the whole resonator might be enlarged with shrinking resonator size in the micrometer size [10]. Further experiments can be conducted to investigate the thermal characteristics of the polymer-filled ring resonators more accurately, based on the numerical models in this study. The results also show that the WGM of a higher order needs a thicker silica capillary to achieve the best sensing performance. So, to assure a large thermal expansion effect of the polymer core, the WGMs of lower orders should be selectively excited for a thinner optimal thickness of the silica capillary. For example, the optimal ring wall thickness of the first-order WGM is smaller than ~2.5 μm, as shown in Fig. 7. Moreover, the WGM of a lower order has a better thermal sensing performance. The theoretical analysis also provides a general guideline for the design and optimization of WGM-resonator-based thermal sensors.

This research is supported by the National Natural Science Foundation of China (NSFC) (grants 90923039 and 51025521) and the 111 Project of China (grant B08043).

References

1. V. Sandoghdar, F. Treussart, J. Hare, V. Lefevre-Seguin, J. M. Raimond, and S. Haroche, "Very low threshold whispering gallery mode microsphere laser," Phys. Rev. A **54**, R1777–R1780 (1996).
2. Y. F. Xiao, C. L. Zou, P. Xue, L. X. Xiao, Y. Li, C. H. Dong, Z. F. Han, and Q. H. Gong, "Quantum electrodynamics in a whispering-gallery microcavity coated with a polymer nanolayer," Phys. Rev. A **81**, 053807 (2010).
3. S. Schiller and R. L. Byer, "High-resolution spectroscopy of whispering gallery modes in large dielectric spheres," Opt. Lett. **16**, 1138–1140 (1991).
4. F. Vollmer and S. Arnord, "Whispering-gallery-mode biosensing: label-free detection down to single molecules," Nat. Methods **5**, 591–596 (2008).
5. N. M. Hanumegowda, C. J. Stica, B. C. Patel, I. M. White, and X. Fan, "Refractometric sensors based on microsphere resonators," Appl. Phys. Lett. **87**, 201107 (2005).
6. N. Lin, L. Jiang, S. M. Wang, L. Yuan, H. Xiao, Y. F. Lu, and H. L. Tsai, "Ultrasensitive chemical sensors based on whispering gallery modes in a microsphere coated with zeolite," Appl. Opt. **49**, 6463–6471 (2010).
7. N. Lin, L. Jiang, S. M. Wang, H. Xiao, Y. F. Lu, and H. L. Tsai, "Thermostable refractive index sensors based on whispering gallery modes in a microsphere coated with poly(methyl methacrylate)," Appl. Opt. **50**, 992–998 (2011).
8. M. Han and A. Wang, "Temperature compensation of optical microresonators using a surface layer with negative thermo-optic coefficient," Opt. Lett. **32**, 1800–1802 (2007).
9. L. He, Y. F. Xiao, C. Dong, J. Zhu, V. Gaddam, and L. Yang, "Compensation of thermal refraction effect in high-*Q* toroidal microresonator by polydimethylsiloxane coating," Appl. Phys. Lett. **93**, 201102 (2008).
10. Q. L. Ma, T. Rossmann, and Z. X. Guo, "Temperature sensitivity of silica micro-resonators," J. Phys. D **41**, 245111 (2008).
11. Q. L. Ma, T. Rossmann, and Z. X. Guo, "Whispering-gallery mode silica microresonators for cryogenic to room temperature measurement," Meas. Sci. Technol. **21**, 025310 (2010).
12. M. L. Corodetsky, A. A. Savchenkov, and V. S. Ilchenko, "Ultimate Q of optical microsphere resonators," Opt. Lett. **21**, 453–455 (1996).
13. B. B. Li, Q. Y. Wang, Y. F. Xiao, X. F. Jiang, Y. Li, L. X. Xiao, and Q. H. Gong, "On chip, high-sensitivity thermal sensor based on high-*Q* polydimethylsiloxane-coated microresonator," Appl. Phys. Lett. **96**, 251109 (2010).
14. C. H. Dong, L. He, Y. F. Xiao, V. R. Gaddam, S. K. Ozdemir, Z. F. Han, G. C. Guo, and L. Yang, "Fabrication of high-*Q* polydimethylsiloxane optical microspheres for thermal sensing," Appl. Phys. Lett. **94**, 231119 (2009).
15. J. R. Schwesyg, T. Beckmann, A. S. Zimmermann, K. Buse, and D. Haertle, "Fabrication and characterization of whispering gallery mode resonators made of polymer," Opt. Express **17**, 2573–2578 (2009).
16. J. D. Suter, I. M. White, H. Zhu, and X. Fan, "Thermal characterization of liquid core optical ring resonator sensors," Appl. Opt. **46**, 389–396 (2007).
17. Y. Sun and X. Fan, "Analysis of ring resonators for chemical vapor sensor development," Opt. Express **16**, 10254–10267 (2008).
18. Y. Sun, S. I. Shopova, G. F. Mason, and X. Fan, "Rapid chemical-vapor sensing using optofluidic ring resonators," Opt. Lett. **33**, 788–790 (2008).
19. C. H. Dong, F. W. Sun, C. L. Zou, X. F. Ren, G. C. Guo, and Z. F. Han, "High-*Q* silica microsphere by poly(methyl methacrylate) coating and modifying," Appl. Phys. Lett. **96**, 061106 (2010).
20. C. F. Bohren and D. R. Huffman, *Absorption and Scattering of Light by Small Particles* (Wiley, 1998).
21. T. Ling and L. J. Guo, "A unique resonance mode observed in a prism-coupled micro-tube resonator sensor with superior index sensitivity," Opt. Express **15**, 17424–17432 (2007).
22. T. Ling and L. J. Guo, "Analysis of the sensing properties of silica microtube resonator sensors," J. Opt. Soc. Am. B **26**, 471–477 (2009).
23. X. D. Fan, I. M. White, H. Y. Zhou, J. D. Suter, and H. Oveys, "Overview of novel integrated optical ring resonator bio/chemical sensors," Proc. SPIE **6452**, 64520M (2007).
24. B. Ozel, R. Nett, T. Weigel, G. Schweiger, and A. Ostendorf, "Temperature sensing by using whispering gallery modes with hollow core fibers," Meas. Sci. Technol. **21**, 094015 (2010).